

# Determination of the rate parameters of N/H/O elementary reactions based on H<sub>2</sub>/O<sub>2</sub>/NO<sub>x</sub> combustion experiments

M. Kovács, T. Varga, C. Olm, Á. Busai, R. Pálvölgyi, I. Gy. Zsély, T. Turányi

*Institute of Chemistry, ELTE Eötvös Loránd University, Budapest, Hungary*

## Introduction

Environmental regulations of industrial processes require the exploration of the behaviour of nitrogen oxides in combustion systems. Several detailed reaction mechanisms [1-17] were published in the last decades to describe the generation of NO<sub>x</sub> in combustion systems. These mechanisms are also applicable to facilitate the development of technologies for lowering NO<sub>x</sub> emission from combustion systems. In a recent review, Glarborg *et al.* [1] state that for all NO<sub>x</sub> formation routes and all major non-catalytic NO removal methods good reaction schemes are available, but the simulation results still have high uncertainty.

In this work, concentration profiles measured in jet stirred reactors, ignition delay times determined in shock tubes, concentration profiles measured in flow reactors, laminar burning velocity measurements and concentration profiles measured in burner stabilized flames (indirect measurements) related to hydrogen–oxygen combustion systems doped with NO, NO<sub>2</sub> or N<sub>2</sub>O, and H<sub>2</sub>/N<sub>2</sub>O combustion systems were considered. These data, together with direct experimental and theoretical determinations of the rate coefficients were used to obtain the rate parameters of ten selected N/H/O elementary reactions with low uncertainty. A methodology was developed by Turányi *et al.* [18] for the determination of rate parameters based on direct and indirect measurements, and theoretical determinations. The method provides rate parameters which are in accordance with the considered indirect measurements and the literature information related to the investigated elementary reactions.

## Collection of experimental data

Our aim was to collect all experimental data on hydrogen combustion influenced with nitrogen oxides related to measurements in homogenous reactors and flames. The summary of the experimental data considered is given in Table 1.

**Table 1.** List of the considered hydrogen combustion experiments.

Experiment	Datasets	Data points	$T / \text{K}$	$p / \text{atm}$	$\phi$
JSR <sup>a</sup>	19	945	700–1150	1–10	0.1–2.5
IDT <sup>b</sup>	65	775	738–2712	0.14–35.9	0.3–5.0
FLOW <sup>c</sup>	43	1538	780–1382	0.5–12.5	0.25–3.77
LBV <sup>d</sup>	7	88	297–299	0.197–1.02	0.15–1.79
BSF <sup>e</sup>	81	1727	293–970	0.026–1	0.45–1.74

<sup>a</sup>JSR: concentration profiles measured in jet stirred reactors; <sup>b</sup>IDT: ignition delay time measured in shock tubes; <sup>c</sup>FLOW: concentration profiles measured in flow reactors; <sup>d</sup>LBV: laminar burning velocity measurements; <sup>e</sup>BSF: concentration profiles measured in burner stabilized flames

All collected indirect experimental data (5073 data points in 215 data sets) were stored in ReSpecTh Kinetics Data (RKD) files. The RKD-format [19,20] was developed from the PrIme kinetics data format [21,22] by adding several new keywords. These data formats are XML based and can be well read by both humans and computer codes. The RKD-format files were created with our *Optima++* code [23]. *Optima++* was also used for reading the data files, running the *FlameMaster* simulation code [24] and comparing the simulation results with the experimental data.

### Selection of a mechanism for the optimisation studies

The experimental data were reproduced using detailed reaction mechanisms developed for the description of NO<sub>x</sub> chemistry in combustion systems. 17 mechanisms listed in Table 2 were considered which are widely used in science and industry. All collected experimental data were simulated with each of the mechanisms.

The obtained simulation results, belonging to different mechanisms, were typically very different from each other and sometimes also from the experimental data. Agreement of the simulation results with the experimental data was investigated using the following objective function.

$$E(\mathbf{p}) = \frac{1}{N} \sum_{i=1}^N \frac{1}{N_i} \sum_{j=1}^{N_i} \left( \frac{Y_{ij}^{\text{mod}}(\mathbf{p}) - Y_{ij}^{\text{exp}}}{\sigma(Y_{ij}^{\text{exp}})} \right)^2 \quad (1)$$

Here  $N$  is the number of datasets and  $N_i$  is the number of data points in the  $i$ -th dataset. Vector  $\mathbf{p}$  contains the rate parameters. Values  $y_{ij}^{\text{exp}}$  and  $\sigma(y_{ij}^{\text{exp}})$  are the  $j$ -th data point and its standard deviation, respectively, in the  $i$ -th dataset.

**Table 2.** The performance of the various reaction mechanisms considered at the reproduction of all experimental data and various subsets of them (see text).

Mechanism	$E_{\text{all}}$	$E_{\text{filtered}}$	$E_{\text{JSR}}$	$E_{\text{IDT}}$	$E_{\text{FLOW}}$	$E_{\text{LBV}}$	$E_{\text{BSF}}$	$E_{\text{common}}$
all data points:	4949	4779	945	625	1481	88	1640	2299
Glarborg-2018 [1]	62.20	17.50	5.57	39.98	7.04	27.93	10.52	7.54
Nakamura-2017 [2]	51.67	12.47	5.47	15.40	7.49	191.19	10.29	7.74
Zhang-2017 [3]	39.31	19.15	6.30	35.43	17.24	17.56	12.57	9.01
POLIMI-2017 [4]	65.83	18.02	17.32	32.29	9.97	37.17	11.03	17.54
Mevel-2009 [5]	89.62	75.69	4.77	146.16	10.38	-	-	23.68
Abian-2015 [6]	150.92	98.27	5.39	208.54	9.01	-	-	32.00
Klippenstein-2011 [7]	151.77	98.70	5.39	211.75	9.01	-	-	32.00
GRI3.0-1999 [8]	65.99	43.46	8.83	109.92	33.18	41.72	10.57	38.49
Okafor-2018 [9]	93.66	64.68	4.98	110.40	33.00	-	-	38.95
Song-2018 [10]	70.19	26.09	110.14	22.57	14.86	73.73	11.17	57.52
SanDiego-2014 [11]	174.27	79.42	24.11	118.41	53.46	-	-	65.31
SanDiego-2018 [12]	151.31	73.80	6.68	104.96	60.36	-	-	69.42
POLIMI-2007 [13]	181.38	116.53	6.62	233.73	26.73	-	-	73.43
Konnov-2009 [14]	143.97	124.21	13.10	182.84	104.67	-	-	98.40
Tian-2009 [15]	113.18	103.76	5.41	146.78	97.05	-	-	98.86
Rasmussen-2008 [16]	116.56	105.55	15.91	129.05	140.78	-	-	116.65
GDFKin-2016 [17]	423.52	364.64	4.31	792.71	18.04	-	-	118.23

The corresponding simulated (modelled) value is  $Y_{ij}^{\text{mod}}$  obtained from a simulation using a detailed mechanism and an appropriate simulation method. If a measured value is characterized by absolute errors (the scatter is independent of the magnitude of  $y_{ij}$ ), then  $Y_{ij} = y_{ij}$ . This option is used for measured concentration profiles and laminar burning velocities. If the experimental results are described by relative errors (the scatter is proportional to the value of  $y_{ij}$ ), then option  $Y_{ij} = \ln(y_{ij})$  is used, which is characteristic for ignition delay time measurements.

We investigated the effect of filtering the influence of less reproducible experimental data. In the “filtered” calculation of the error function all experimental datasets were excluded, which provided larger than  $E = 100$  values for all of the Glarborg-2018, Nakamura-2017, Zhang-2017 and POLIMI-2017 mechanisms (13 datasets were excluded out of 215). Comparing the  $E_{\text{all}}$  and  $E_{\text{filtered}}$  columns of Table 2 shows that excluding these datasets resulted in much lower  $E$  values for most mechanisms.  $E_{\text{common}}$  is a result of a further filtering when we take into account only those datasets which have been simulated successfully with all the mechanisms.

Based on the results presented in Tables 2, the Glarborg-2018 mechanism was selected for further investigations.

### The optimisation method

Local sensitivity analysis was used to identify the most important elementary reactions at the conditions of the experiments. A reaction was considered important at a data point if the absolute value of the sensitivity coefficient was larger than 10% of the absolute value of the largest sensitivity coefficient. Important reactions were assigned to each dataset based on the importance of reactions at the data points. Only the important N/H/O reactions were looked for, since the rate parameters of the H/O subset have been optimised in our previous work [25]. The selected reactions are listed in Table 3. The optimal rate parameters are also shown in the table which were determined with our optimisation method described below.

**Table 3.** List of reactions selected for optimisation and the optimised rate parameters. Units are  $\text{cm}^3$ , mol, s, K. LP stands for low pressure limit.

R. number	Reaction	$A$	$n$	$E/R$
R1	$\text{NO}_2 + \text{H} = \text{NO} + \text{OH}$	$1.70 \cdot 10^{14}$	$-6.72 \cdot 10^{-3}$	$1.65 \cdot 10^2$
R2	$\text{NO} + \text{HO}_2 = \text{NO}_2 + \text{OH}$	$2.58 \cdot 10^{12}$	$-2.63 \cdot 10^{-2}$	$-2.12 \cdot 10^2$
R3 LP	$\text{NO} + \text{H} + \text{M} = \text{HNO} + \text{M}$	$7.47 \cdot 10^{15}$	$-1.85 \cdot 10^{-1}$	$-4.23 \cdot 10^2$
R4 LP	$\text{N}_2\text{O} + \text{M} = \text{N}_2 + \text{O} + \text{M}$	$7.36 \cdot 10^{27}$	-3.45	$3.56 \cdot 10^4$
R5	$\text{NO}_2 + \text{H}_2 = \text{HONO} + \text{H}$	$1.26 \cdot 10^4$	2.78	$1.48 \cdot 10^4$
R6 LP	$\text{NO} + \text{O} + \text{M} = \text{NO}_2 + \text{M}$	$1.07 \cdot 10^{20}$	-1.42	$1.40 \cdot 10^2$
R7	$\text{N}_2\text{O} + \text{H} = \text{N}_2 + \text{OH}$	$9.82 \cdot 10^{13}$	$-3.86 \cdot 10^{-2}$	$6.62 \cdot 10^3$
R8 LP	$\text{NO} + \text{OH} + \text{M} = \text{HONO} + \text{M}$	$5.49 \cdot 10^{21}$	-1.92	$-2.03 \cdot 10^2$
R9	$\text{HONO} + \text{OH} = \text{NO}_2 + \text{H}_2\text{O}$	$2.76 \cdot 10^{10}$	$5.70 \cdot 10^{-1}$	$-2.63 \cdot 10^2$
R10	$\text{NO}_2 + \text{H}_2 = \text{HNO}_2 + \text{H}$	$3.32 \cdot 10^2$	2.97	$1.51 \cdot 10^4$

The global parameter optimisation method applied here has been described in detail by Turányi *et al.* [18]. The optimal set of rate parameters was obtained by the minimization of objective function Eq. (1). The optimal rate parameters were looked for in such a way that the calculated rate coefficients always remained within their prior uncertainty bands. The determination of the covariance matrix of the optimised parameters (“posterior covariance matrix”) and the calculation of the temperature dependent uncertainties of the optimised rate coefficients have been described in detail in [18].

Results of this work are new recommended Arrhenius parameters of the investigated ten elementary reactions. These values are based on a large set of data (1639, 624 and 131 data points in 69,

39, 9 data sets of indirect measurements, direct measurements and theoretical determinations, respectively). Altogether 2394 data points in 117 datasets were utilized. The obtained Arrhenius parameters are given in Table 3.

Reactions R2 and R6 were selected to present the initial and optimised rate coefficient – temperature functions and to compare the prior and posterior uncertainty bands. Figure 1. shows that the posterior uncertainty band of the rate coefficients obtained as a result of fitting the rate parameters to large number of data points is usually much narrower than the prior uncertainty band, obtained from processing the literature information. For most reactions the optimised rate coefficients are in good agreement with the selected direct measurements and theoretical determinations.

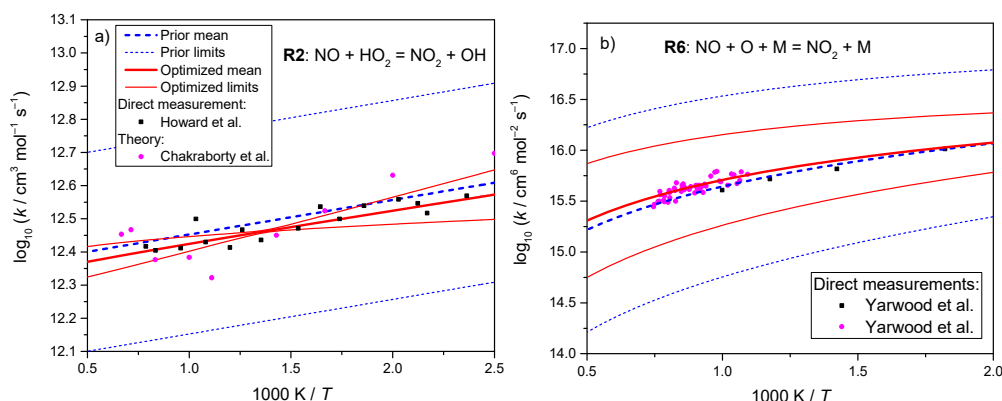


**Figure 3.** The Arrhenius-plots of the initial and optimised rate parameters and the related prior and posterior uncertainty limits, respectively, for reactions a) R2 and b) R6.

## References

- [1] P. Glarborg *et al.*, *Progress in Energy and Combustion Science* **67** (2018) 31-68
- [2] H. Nakamura *et al.*, *Combustion and Flame* **185** (2017) 16-27
- [3] Y.J. Zhang *et al.*, *Combustion and Flame* **182** (2017) 122-141
- [4] T. Faravelli, POLIMI-2017 (NOx\_170728), Personal communication, (2017)
- [5] R. Mevel *et al.*, *Proceedings of the Combustion Institute* **32** (2009) 359-366
- [6] M. Abian *et al.*, *International Journal of Chemical Kinetics* **47** (2015) 518-532
- [7] S.J. Klippenstein *et al.*, *Combustion and Flame* **158** (2011) 774-789
- [8] G.P. Smith *et al.*, GRI-Mech 3.0, [http://www.me.berkeley.edu/gri\\_mech/](http://www.me.berkeley.edu/gri_mech/)
- [9] E.C. Okafor *et al.*, *Combustion and Flame* **187** (2018) 185-198
- [10] Y. Song *et al.*, *Proceedings of the Combustion Institute*, **37**, in press (2018)
- [11] San Diego Mechanism version 2014-10-04 <http://combustion.ucsd.edu>
- [12] San Diego Mechanism version 2018-07-23 <http://combustion.ucsd.edu>
- [13] A. Frassoldati *et al.*, *International Journal of Hydrogen Energy* **32** (2007) 3471–3485
- [14] A.A. Konnov *Combustion and Flame* **156** (2009) 2093–2105
- [15] Z. Tian *et al.*, *Combustion and Flame* **156** (2009) 1413-1426
- [16] C.L. Rasmussen *et al.*, *Combustion and Flame* **154** (2008) 529-545
- [17] N. Lamoureux *et al.*, *Combustion and Flame* **163** (2016) 557-575
- [18] T. Turányi *et al.*, *International Journal of Chemical Kinetics* **44** (2012) 284–302
- [19] T. Varga *et al.*, *Proceedings of the 7th European Combustion Meeting* (2015) P1-04
- [20] ReSpecTh webpage, <http://respecth.hu>
- [21] M. Frenklach, *Proceedings of the Combustion Institute* **31** (2007) 125–140
- [22] M. Frenklach, PrIme Webpage, <http://www.primekinetics.org/>
- [23] Á. Busai. T. Varga, Optima++ v1.01, <http://respecth.hu>
- [24] H. Pitsch, FlameMaster v4.0, <https://www.itv.rwth-aachen.de/>
- [25] T. Varga *et al.*, *International Journal of Chemical Kinetics* **48** (2016) 407–422